APPLIED ORGANOMETALLIC CHEMISTRY, VOL. 10, 637–647 (1996)

Charge Transport in Mesomorphic Phthalocyanines Studied by Pulse-Radiolysis Time-Resolved Microwave Conductivity

John M. Warman* and Pieter G. Schouten
IRI, Delft University of Technology, Mekelweg 15, 2629 JB Delft, The Netherlands

The pulse-radiolysis time-resolved microwave conductivity (PR-TRMC) technique has been used to obtain information on the transport of charge within columnarly stacked, peripherally octaalkoxy-substituted phthalocyanines. Data are presented on the one-dimensional, intracolumnar charge mobility and on the timescale of quasi-two-dimensional intercolumnar electron tunnelling. Particular attention is paid to materials that are liquid-crystalline at room temperature, because of their potential technological importance in optoelectric charge transport layers and molecular semiconductor devices. The relevance of the data to channeled charge transport in aligned thin layers is discussed.

Keywords: phthalocyanines; discotic liquid crystals; optoelectric materials; molecular semiconductors; charge transport; pulse radiolysis; microwave conductivity; electron tunneling; molecular electronics; molecular wires.

INTRODUCTION

Disk-shaped aromatic macrocycles, when peripherally substituted with long alkyl chains, display a tendency to assemble into columnar aggregates with the macrocycle forming the core and the alkyl chains forming an insulating mantle between the cores. These compounds often display thermotropic mesomorphism with extended regions of temperature over which they have liquid-crystalline properties.[1–3] A particularly important class of these discotic liquid-crystalline materials are the peripherally octa-substituted phthalocyanines (PcR_8), first synthesized by Simon and co-workers[4] and the subject of recent reviews.[5–8] The potential technological importance of these compounds lies in their semiconductive properties with a relatively small bandgap of *ca* 2 eV,[9,10] combined with their excellent thermal and radiation stability, and malleability in the liquid-crystalline state. Of particular importance for applications in charge transport layers and molecular electronic devices are the one-dimensional, coaxial nature of conduction and the possibility of controlling the alignment of the columns by mechanical or magnetic means.[11–19]

At room temperature most PcR_8 derivatives form crystalline solids which are technologically unsuitable because of the inevitable presence of grain boundaries which form barriers to bulk charge motion. The extension of the mesomorphic properties down to ambient temperatures is therefore a prerequisite for many applications. Two methods of achieving this have been found for octa-alkoxy–substituted phthalocyanines (PCs). The first involves the polymerization of the dihydroxysilicon monomer to form a phthalocyaninato-polysiloxane.[7,19–25] The second involves the incorporation of methyl branches in the peripheral alkyl chains.[19,26,27]

In this paper we present data on the charge transport properties of such room-temperature mesomorphic alkoxy derivatives and compare them with those of monomeric n-alkoxy compounds. The structures of the compounds are shown in Fig. 1. As can be seen, the liquid-crystalline phase is characterized by horizontal columnar stacking of the macrocycles, as opposed to tilted stacking in the crystalline solid.

Of prime interest are properties such as the one-dimensional mobility of charge along the 'conducting' macrocyclic cores of the columns, and the exchange of charge between columns ('crosstalk') resulting from electron tunneling through the 3 eV barrier presented by the saturated hydrocarbon mantle. The latter process

* Author to whom correspondence should be addressed.

CCC 0268–2605/96/080637–11

Received 25 April 1995
Accepted 30 April 1995

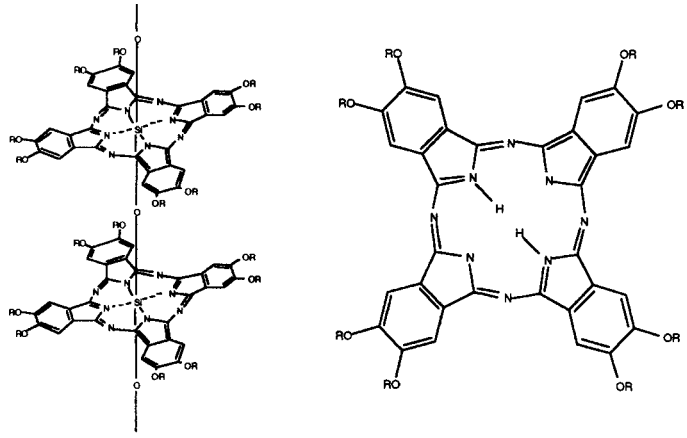

Figure 1 The primary molecular and secondary columnar structures of the peripherally octa-alkoxy-substituted phthalocyanines discussed. The polymeric compound is denoted $(Si(OcOC8)O)_n$ in the text. The monomeric compounds are denoted PcOC*n*,*m* with *n* the length of the alkyl chain and *m* the number of methyl branches.

represents the limiting factor in what would otherwise be perfectly channeled charge transport down to molecular dimensions.

The bandgap of *ca* 2 eV results in an extremely small concentration of intrinsic electronic charge carriers. The pure materials are consequently insulators with background conductivities much less than 10^{-10} S m^{-1}.[8,28] Therefore, in order to investigate their electronic properties it is necessary to introduce charge carriers artificially. This is most frequently achieved by chemical doping with strong redox agents such as iodine. The disadvantage is that the actual concentration of charge carriers is usually unknown and, for the high dopant concentrations often used, the secondary, columnar, structure of the material can be considerably perturbed.[29]

Photoionization is limited by the extremely small penetration depth of photons of super-bandgap energies. However, this can be turned to advantage in time-of-flight (TOF) measurements of charge carrier mobilities. This type of measurement requires the availability of single crystals or well-aligned liquid-crystalline materials and the use of ohmic electrode contacts. At this time no TOF measurements on mesomorphic phthalocyanines appear to have been reported, but TOF measurements of charge carrier mobilities on the order of 10^{-4} m^2 V^{-1} s^{-1} have been made on single crystals of phthalocyanine itself.[30,31] Very recently TOF measurements on related mesomorphic triphyenylene derivatives were carried out.[32–34] These have shown that charge carrier mobilities on the order of 10^{-6} m^2 V^{-1} s^{-1} or even higher can prevail in orthogonally aligned samples of discotic liquid-crystalline films. This is more than three orders of magnitude larger than the mobilities found for the doped amorphous polymers being used at present as charge transport layers.[35]

The recent TOF mobilities are similar in magnitude to those previously reported using the present PR-TRMC technique.[27,36–38]

In the PR-TRMC approach, short (nanosecond)-duration pulses of high-energy radiation are used to ionize bulk samples of the material of interest. The penetration depth is much larger than the sample thickness, resulting in electron–hole pairs being distributed uniformly throughout the medium. The pulse-radiolysis procedure has been referred to as 'radiation doping'. The particular advantages of pulse radiolysis for this type of study are (a) the ultrashort formation and observation time; (b) the uniform, very low (ppm) concentration of carriers formed, which does not perturb the molecular structure; and (c) the accurate knowledge of the energy absorbed which allows estimates to be made of the charge carrier concentration.

If the electrons and/or holes are mobile, then the conductivity of the material will increase as a result of the ionizing pulse. The radiation-

induced conductivity is measured by monitoring the change in microwave power reflected by the sample cell.

The advantages of the use of microwaves for monitoring the radiation-induced conductivity are (a) the absence of the necessity of ohmic contacts, (b) applicability to polycrystalline samples, (c) the absence of polarization and space-charge effects, and (d) the absence of domain or grain boundary effects. With regard to the last point, it is important to emphasize that the microwaves used, with frequencies of several gigahertz and field strengths of only a few volts per centimeter, result in only a very small and rapidly alternating perturbation of the normal random diffusional motion of charge carriers within organized domains of the sample. The mobility derived should therefore give an estimate of the maximum mobility that could be achieved in a d.c. field for a sample which is perfectly orthogonally aligned between the electrodes, after an upward correction by a factor of approximately 3 to correct for the fact that the directions of the domains are oriented isotropically in the PR-TRMC measurements.

A major disadvantage of the present technique is that only the sum of the positive and negative charge carrier mobilities can be derived; it is therefore impossible to determine the individual mobilities of electrons and holes. Although TOF measurements have shown holes to be the major charge carriers in the triphenylene derivatives, this is not necessarily the case for PC derivatives. For unsubstituted phthalocyanine, electrons and holes have in fact been found to have closely similar mobilities.[30, 31]

Below we present an outline of the application of the PR-TRMC method to the study of charge migration in discotic liquid-crystalline compounds and the possible relevance of the data obtained to the properties of these materials as charge transport layers.

MATERIALS

Figure 1 shows the primary molecular structure of the compounds studied in the present work. The synthesis and characterization of these materials have been described previously.[19, 23, 26, 39–42]

The monomeric n-alkoxy-substituted derivatives all precipitate from solution as crystalline powders at room temperature and undergo a transition from the crystalline solid, K, to a liquid-crystalline mesophase, D, on heating. The K→D transition temperatures, as obtained by differential scanning calorimetry, are given in Table 1. The transition is reversible with a hysteresis of approximately 25 °C. Small-angle X-ray diffraction, SAXS, shows the molecules to be columnarly stacked in both phases with a tilted arrangement in the K phase resulting in oblique packing of the columns and a Pc-to-Pc distance along the columnar axis of approximately 4.3 Å. In the mesophase a SAXS pattern characteristic of hexagonal packing and a reflection corresponding to a distance of 3.4 Å show that the molecules are horizontally stacked with respect to the columnar axis. The intercolumnar center-to-center distances, D, calculated from the hexagonal lattice parameters are listed in Table 1.

Table 1 Solid-to-mesophase and mesophase-to-isotropic liquid transition temperatures determined by DSC, and intercolumnar distances in the D_h mesophase determined by SAXS

Compound	$T_{K\rightarrow D}$ (°C)	$T_{D\rightarrow I}$ (°C)	D (Å)	Reference
PcOC6	119	>350	27.6	41
	102			5
PcOC9	101	>350	31.4	41
	107			27
PcOC12	83	309[c]	35.2	41
	91			5.57
PcOC8,2	70[a]	295	32.0	19
PcOC8,2*	—[b]	295	31.6	26
PcOC12,3	—[b]	185	34.4	19
[Si(PcOC8)0]$_n$	—[b]	—	28.5	23

[a] Metastable mesophase is obtained on cooling.
[b] No evidence for a crystalline solid phase down to −100 °C.
[c] Accompanied by decomposition.

The PcOC8,2 compound with two methyl branches also precipitates from solution at room temperature as a crystalline solid but with an intracolumnar spacing of 3.48 Å, which is close to the cofacial contact distance of 3.4 Å for aromatic π-systems, therefore indicating close-to-horizontal columnar stacking of the molecules and hexagonal packing of the columns even in the K-phase. DSC and SAXS show PcOC8,2 to undergo a transition to a liquid-crystalline phase at 70 °C; this phase can be supercooled to −100 °C with no sign of recrystallization. When

it is allowed to stand for several hours at room temperature recrystallization does gradually take place, however.

When PcOC8,2 was synthesized with one enantiomer of the branched alkoxy chain, denoted PcOC8,2*, the material proved to be liquid-crystalline even on precipitation from solution at room temperature.[26] No evidence could be found for a D→K transition at lower temperatures. At 80 °C the 3.4 Å SAXS reflection displays satellites suggesting a helical superstructure within the columns with a periodicity of 16 molecules. Both PcOC8,2 and PcOC8,2* undergo a transition to an isotropic liquid phase at 295 °C.

The triply branched PcOC12,3 compound precipitates at room temperature as a horizontally stacked, liquid-crystalline solid. No evidence for a D→K transition could be found down to −100 °C. PcOC12,3 has a very low clearing temperature of 185 °C and can be readily aligned.[19] These properties make it a particularly attractive candidate for thin-layer applications.

The polysiloxane compound was obtained by thermal polymerization of the silanediol monomer at 200 °C in its hexagonal discotic mesophase.[23,42] The hexagonal packing, with horizontal stacking of the molecules, is retained on cooling to room temperature. No evidence is found for crystallization on cooling to as low as −100 °C. The average degree of polymerization is estimated to be approximately 100 on the basis of measurements on the related $[Si(PcOC12)O]_n$ compound.[42]

EXPERIMENTAL

The pulse-radiolysis time-resolved microwave conductivity, PR-TRMC, technique has been fully described elsewhere.[43–45] The materials are contained in a microwave cell which consists of a piece of rectangular waveguide of cross-section 7.1 mm × 3.55 mm closed at one end with a metal plate. Approximately 200 mg of material is compressed into the cell using a close-fitting Teflon rod, then the weight and length of the sample are measured. The temperature of the cell can be varied over the range of −100 to +200 °C. When less material is available, use is made of a Perspex block with a rectangular 2 mm × 6 mm × 3 mm cavity which can be filled with approximately 25 mg of material. The Perspex block is then placed in the microwave cell. When it is used, the upper temperature is limited to 120 °C.

The samples are ionized by pulsed irradiation with 3 MeV electrons from a Van de Graaff accelerator using pulse widths of 2–50 ns. The integrated beam charge per pulse, Q(nC), is monitored routinely. The range of a 3 MeV electron is 15 mm in a medium of density 1 g cm^{-3}, resulting in almost uniform energy deposition throughout the sample of $0.58Q$ J kg^{-1}. A single 10 ns pulse results in the formation of approximately 10^{-5} molar $(6\times10^{21}$ m$^{-3})$ e^-h^+ pairs.

Microwaves within the frequency range 26.5–38 GHz were produced by a Gunn diode oscillator (Midcentury) at an average power level of *ca* 100 mW. Changes in the microwave power reflected by the cell were detected using a Schottky barrier detector diode, the output of which was monitored using either a Tektronix 7912 digitizer with a time resolution of 1 ns or a tandem combination of a Tektronix 2205 oscilloscope (7A13 plug-in) and a Sony/Tektronix RTD digitizer capable of monitoring data points from 10 ns to 10 ms on a pseudologarithmic timebase following a single radiation pulse. Examples of the radiation-induced conductivity transients obtained by both methods are shown in Fig. 2.

The change in microwave power reflected, ΔP_R, is directly related to the radiation-induced conductivity (Eqn [1]).

$$\Delta\sigma = A\Delta P_R/P_R \qquad [1]$$

The proportionality factor A can be calculated, thus allowing an absolute determination of $\Delta\sigma$.[44–46] Conductivity changes were usually on the order of 10^{-4} to 10^{-3} S m^{-1}.

RESULTS AND DISCUSSION

As has been fully discussed previously,[27,39,46,47] the physical model which best describes the experimental observations is one in which the charge carriers responsible for the radiation-induced conductivity originate as electron–hole pairs formed by ionization events within the hydrocarbon tail regions. During the course of mutual diffusional motion a fraction of these pairs undergoes electron and hole scavenging by

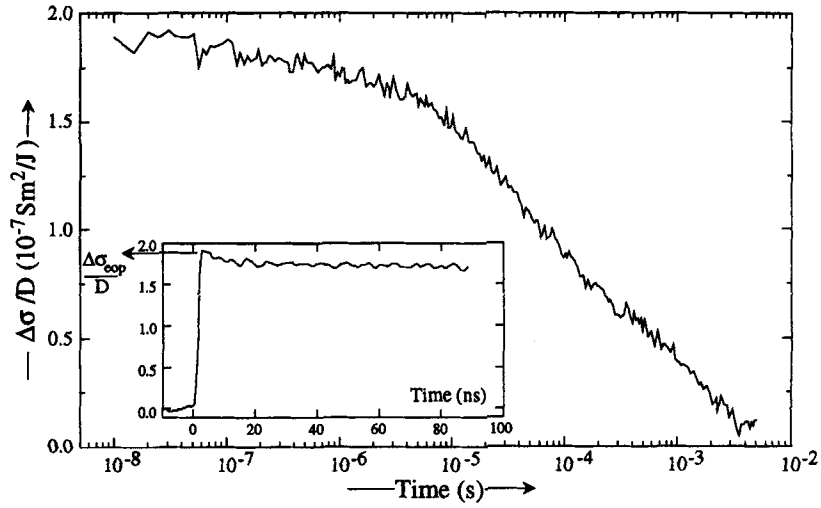

Figure 2 Radiation-induced microwave conductivity transients for PcOC12 as monitored by the PR-TRMC technique using a 2 ns, 4 A pulse of 3 MeV electrons. The inset was taken on a linear timescale using a Tektronix 7912 digitizer. The main trace was obtained using a single pulse on a pseudologarithmic timescale from 10^{-8} to 10^{-2} s using a SonyTektronix RTD 710 recorder. From the end-of-pulse conductivity, information is obtained on the intracolumnar charge carrier mobility or jump time τ_J. From the decay of the conductivity, information is obtained on intercolumnar charge recombination via electron tuneling with a time τ_T.

the Pc cores of separate stacks in competition with their geminate recombination. The elongated lifetime of these core-localized carriers results from the fact that the electron affinity of phthalocyanine (3 eV)[9] is much larger than that of the surrounding alkane mantle (*ca* 0 eV)[48] and the PC ionization potential (5 eV)[9] is much lower (*ca* 8 eV for the surrounding alkane).[49,50] The barriers to intercolumnar electron and hole transfer will therefore both be very large, at approximately 3 eV. Charge recombination can then only occur via long-distance, through-bond assisted tunneling through the hydrocarbon mantle. While localized on a Pc stack, the charge carriers are still one-dimensionally mobile along the core axis due to rapid hopping between macrocyclic units. This motion is responsible for the conductivity observed.

Two separate pieces of information can be obtained from PR-TRMC transients such as those shown in Fig. 2. From the dose-normalized end-of-pulse conductivity, $\Delta\sigma_{eop}/D$, the intracolumnar mobility and hence the jump or hopping time, τ_J, can be estimated. From the eventual decay of the conductivity, estimates can be made of the timescale of intercolumnar electron tunneling or 'crosstalk' between columns. These aspects will be presented separately below, before the possible relevance of the parameters obtained to charge transport in organized layers is discussed.

End-of-pulse conductivity/ Intracolumnar charge-hopping

As shown previously,[27,37] the dose-normalized end-of-pulse conductivity is directly related to the sum of the intracolumnar charge carrier mobilities, $\Sigma\mu=[\mu(+)+\mu(-)]$ (Eqn 2):

$$[\Delta\sigma_{eop}/D]=W_{eop}\sum \mu/E_p \qquad [2]$$

E_p is the average energy required to form one initial e^-h^+ pair, in electronvolts. The value can be estimated from the bandgap energy, E_G, using the relationship derived by Alig et al (Eqn 3):[51]

$$E_P \approx 2.73E_G+0.50 \text{ [eV]} \qquad [3]$$

Since the charge carriers responsible for the long-lived conductivity signals observed in the present materials are thought to originate in the saturated hydrocarbon regions,[27,39,47] for which $E_G \approx 8.5$ eV, the value of E_P is uusually taken to be approximately 25 eV. E_P should be independent of temperature or phase changes in the medium.

W_{eop} is the probability that an initial e^-h^+ pair formed within the pulse survives to the end of the pulse, i.e. does not undergo subnanosecond charge recombination or trapping. W_{eop} has a *maximum* value of 1 and would be expected to be only weakly dependent on temperature.[27] In view of this, the experimental parameter $[\Delta\sigma_{eop}/D)$ should closely reflect changes in the charge carrier mobility alone.

In Fig. 3 $[\Delta\sigma_{eop}/D]$ is plotted as a function of temperature for the heating and cooling cycles of PcOC12 and $[Si(PcOC8)O]_n$. The sudden drop in $[\Delta\sigma_{eop}/D]$ at the K→D transition for the monomeric n-alkoxy compound is clearly apparent and is attributed to the perturbation of charge transport resulting from the greatly increased motional freedom in the mesophase compared with the crystalline solid. Any increase in mobility which might have been expected to result from the change from a tilted to a horizontal configuration of the macrocycles appears to be overcompensated for by the motional freedom which will cause rotational, longitudinal and lateral fluctuations in the columnar order.

The values for the siloxane polymer are seen to be very similar to those for the monomeric material in its mesophase, as would be expected. Also, in agreement with the lack of observation of DSC transients, the polymer shows only a gradual, continuous decrease in $[\Delta\sigma_{eop}/D]$ down to -100 °C.

In Figure 4, data are shown for the methyl-branched compounds. Freshly precipitated PcOC8,2 displays a sharp decrease at elevated temperatures similar to that found for PcOC12, in agreement with the conclusion that this compound is initially crystalline. On cooling, however, no abrupt return to the level of the K phase is observed, even down to -100 °C, indicating supercooling of the mesophase. The properties gradually return to those of the crystalline solid on standing for several hours at room temperature.

Both the optically pure PcOC8,2* and PcOC12,3 compounds show no indication in their $\Delta\sigma_{eop}/D$ versus T behavior of a crystalline phase at any temperature, in agreement with DSC and SAXS data. The conductivity in the helical phase of PcOC8,2* is seen to be substantially lower than that for the mixed enantiomer PcOC8,2.

In the case of PcOC12,3 it was possible to study the transition from the mesophase to the isotropic liquid within the temperature range of the PR-TRMC measurements. The sudden decrease by approximately an order of magnitude at the clearing temperature can be seen in Fig. 4. This decrease is to be expected on disruption of the columnar structure and has previously been reported for analogous porphyrin[36] and triphenylene[32–34] materials.

In order to derive absolute mobility values from $\Delta\sigma_{eop}/D$, the pair formation energy, E_P, and survival probability, W_{eop}, must be estimated. Taking 25 eV for E_P, the two values of the mobility at room temperature are given in Table 2: $\Sigma\mu_{min}$, for which the maximum possible value

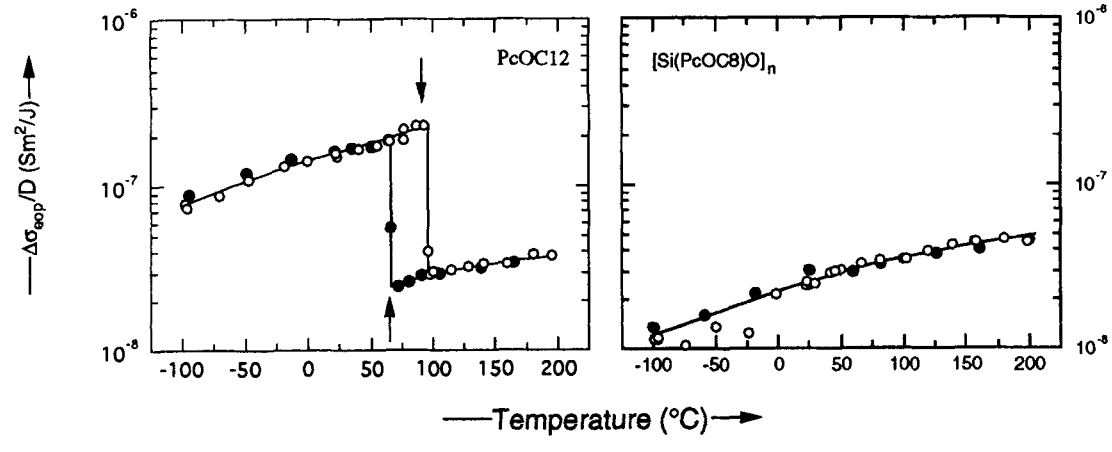

Figure 3 The temperature dependence of the end-of-pulse conductivity for the n-alkoxy compound PcOC12 (left) and the polysiloxane $(Si(PcOC8)O)_n$ compound (right). The open circles are on heating and the filled circles on cooling. The arrows show the temperatures of K↔D transitions as measured by DSC.

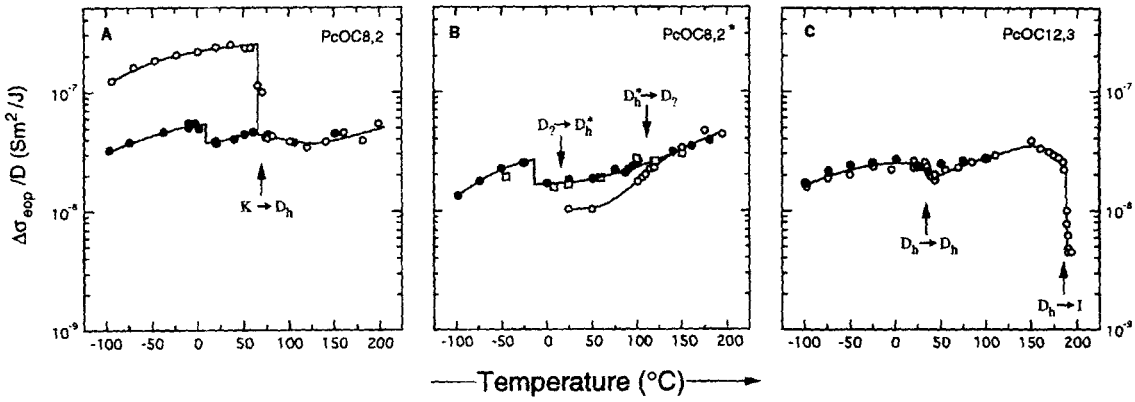

Figure 4 The temprature dependence of the end-of-pulse conductivity for the branched chain compounds PcOC8,2 (left), PcOC8,2* (middle) and PcOC12,3 (right). The open circles are on heating and the filled circles on cooling. The squares in the middle graph are for a second heating cycle. The arrows show the positions of phase transitions as seen by DSC.

of $W_{eop}=1$ was taken; and $\Sigma\mu_s$,for which an estimate of W_{eop} has been made on the basis of scavenging theory.[27,39] Since the domains in the present bulk samples are expected to be aligned randomly, the mobility values would be expected to be lower by a factor of approximately 3 than the one-dimensional mobility in the direction of the axis of the stacks. From the data in Table 2 one can conclude that one-dimensional mobilities close to 0.1×10^{-4} m^2 V^{-1} s^{-1} may be achievable in the orthogonally aligned mesophase of PcOC*n* materials. Mobilities much larger than this are considered to be extremely unlikely.

The order of magnitude of the mobility values, i.e. $\ll10^{-4}$ m^2 V^{-1} s^{-1}, indicates the charge to be mainly localized on individual Pc macrocyclic units and to move via electron exchange between neighboring macrocycles. Accordingly, the site-to-site jump or hopping time τ_j is related to the (three-dimensional) mobility and the jump distance d_j (Eqn [4]):

$$\tau_j \approx ed_j^2/6k_BT\mu \qquad [4]$$

In Table 2 the jump times at room temperature are given based on a jump distance equal to the centre-to-centre distance between Pc macrocycles along the axis of the stack, i.e. 3.4 Å for

Table 2 Charge carrier mobilities, $\Sigma\mu=[\mu(+)+\mu(-)]$, intracolumnar jump times, τ_j, and intercolumnar tunneling times, τ_T, as determined from PR-TRMC transients at room temperature

Compound	$\Sigma\mu_{min}$[a] (10^{-6} m^2 V^{-1} s^{-1})	$\Sigma\mu_s$[b] (10^{-6} m^2 V^{-1} s^{-1})	τ_j (fs)	τ_T (μs)
Crystalline solid				
PcOC6	1.8	6.8	180	0.2
PcOC9	3.9	10.0	120	3.5
PcOC12	3.7	9.1	140	20
PcOC8,2[c]	5.5	12.4	65	0.15
Liquid crystal				
PcOC8,2[d]	1.0	2.3	340	10
PcOC8,2*	0.5	0.9	860	15
PcOC12,3	0.6	1.3	590	300
[Si(PcOC8)O]$_n$	0.6	1.5	150	400

[a] From $\Delta\sigma_{eop}D$ with $E_p=25$ and $W_{eop}=1$.
[b]With W_{eop} calculated[27].
[c]Fresh precipitate.
[d]Metastable room temperature mesophase.

the mesophase, and taking $\Sigma\mu_s$ to be the mobility of the major charge carrier. On the basis of the recent TOF measurements on triphenylenes,[32–34] this would be expected to be the hole. On the basis of single-crystal phthalocyanine TOF measurements,[30,31] electrons and holes would be expected to have similar mobilities, in which case the jump times of each would be approximately twice those listed in the Table.

As can be seen, the jump times in the crystalline solids are on the order of 100 fs. Interestingly the value for the horizontally stacked PcOC8,2 in its room-temperature crystalline phase is significantly shorter than for the tilted stacks of the n-alkoxy derivatives, suggesting that horizontal stacking may indeed have a positive influence on charge migration, all other factors being equal. The values of τ_j in the liquid-crystalline materials are seen to be longer by a factor of approximately 5, at *ca* 500 fs.

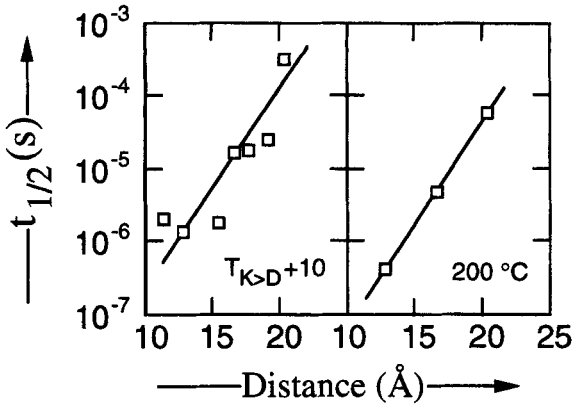

Figure 6 A semi-logarithmic plot of the first half-life of the conductivity decay against the nearest-neighbor edge-to-edge distance between Pc cores in the mesophase of n-alkoxy PcOC*n* compounds at *ca* +10 °C above the phase transition (n=5, 6, 8, 9, 10, 11, 12) and at *ca* 200 °C (n=6, 9, 12).

Conductivity decay/intercolumnar electron tunneling

As can be seen in Fig. 2, the radiation-induced conductivity eventually decays back to zero. For the n-alkoxy derivatives the timescale of this decay has been found to increase exponentially with alkyl chain length.[39,46,47] This effect is illustrated for the liquid-crystalline phase of the n-alkoxy PcOC*n* compounds in Figs 5 and 6. The process responsible has been ascribed to charge recombination controlled by intercolumnar electron tunneling through the saturated hydrocarbon mantle. Because the decays are non-exponential, i.e. not characterized by a single, time-independent rate coeffiicent, we take the first half-life to be a phenomenological measure of the intercolumnar tunneling time, τ_T. Since the barriers towards electron and hole tunneling are similar at *ca* 3 eV, the intercolumnar tunneling times for electrons and holes may be expected to be similar and close to the value of τ_T determined. For a series of n-alkoxy compounds, τ_T in the mesophase has been found to be given by (Eqn [5]):[47]

$$\tau_T \approx 6\times 10^{-13}\exp[0.21(\text{eV})/k_BT]\exp[0.64R(\text{Å})] \quad [5]$$

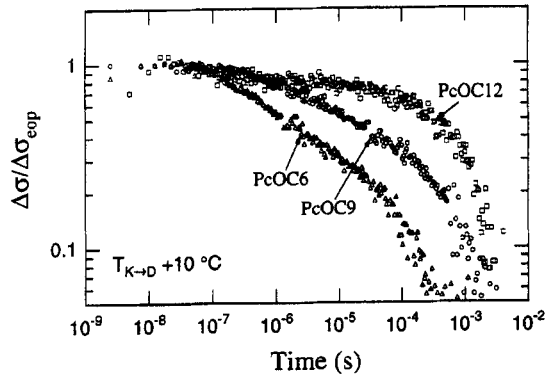

Figure 5 The decay of the conductivity following pulsed irradiation of PcOC6, PcOC9, and PcOC12 in the liquid-crystalline phase at 10°C above the K→D phase transition, i.e. at *ca* 100 °C.

In Table 2 we list the experimental τ_T values determined at room temperature. The dramatic effect of chain length can be seen for the n-alkoxy compounds. Also of interest is the decay time for the supercooled mesophase of the PcOC8,2 compound, which is two orders of magnitude longer than its crystalline solid form. This illustrates the importance of the molecular composition and conformation of the barrier, in addition to the barrier width and height which are the only parameters which appear in the 'classical', through-space tunneling expression. Clearly disorder in the hydrocarbon barrier region retards long-distance electron transfer, as would be expected on the basis of presently favored 'through-bond' or 'superexchange' theories of electron tunneling.[52–56]

Relevance to charge transport materials or devices

Phthalocyanine derivatives are well known for their resistance to thermal and radiation degradation. The additional properties of one-dimensional semiconductivity and room-temperature liquid crystallinity associated with the columnar discotic compounds makes them ideally suited for charge transport materials and for inclusion in molecular electronic devices.

Important general considerations in the vectorial transport of charge are (a) the time for traversal of a given distance Δ under influence of a potential V: the 'drift time' t_D; (b) the temporal dispersion in the drift time caused by longitudinal and transverse diffusion during transport; (c) the spatial dispersion in the image of a point source of charge caused by transverse diffusion, i.e. diffusion perpendicular to the applied field.

Figure 7 is a schematic representation of a layer of orthogonally aligned discotic molecules between two electrodes with charge being injected photolytically in a thin layer. The purpose of the figure is to illustrate the relationship between the parameters τ_j and τ_T determined in the PR-TRMC experiments and the motion of charge through such a layer.

The longitudinal, one-dimensional diffusion coefficient and mobility D_L and μ_L, are related to τ_j (Eqns [6] and [7]).

$$D_L = d_j^2/2\tau_j \quad [6]$$

and

$$\mu_L = ed_j^2/2k_BT\tau_j \quad [7]$$

From the latter parameter the drift time t_D is given by Eqn [8]:

$$t_D = 2\tau_j(k_BT/Ve)\,(\Delta/d_j)^2 \quad [8]$$

At room temperature, for d_j equal to the cofacial contact distance between aromatic molecules of 3.4 Å, Eqn [8] becomes

$$t_D = 4.3\times10^{17}\tau_j\Delta^2/V \quad [9]$$

A jump time of 500 fs would therefore result in a drift time of 200 ns for a layer 1 μm thick with a potential of 1 V across. The drift times for hypothetical, perfectly orthogonally aligned layers of the compounds studied in the present work as estimated from the τ_j values in Table 2 are listed in Table 3.

The very short values of τ_D for the crystalline materials will most probably be unattainable in bulk layers due to grain boundary effects. However, they might be achievable in nanoscale molecular devices. The drift times estimated for the liquid-crystalline PcOC*n* materials are, in general, orders of magnitude shorter than those attainable with presently used donor-doped amorphous plastics, indicating that a substantial gain in speed could be achieved using mesomorphic PcOC*n* compounds.

In addition to the short transit times, it is to be expected that lateral spatial dispersion will be significantly less in aligned discotic layers which intrinsically function as charge channeling devices. Thus diffusion perpendicular to the direction of charge transport should be greatly reduced due to charge confinement by the coaxial hydrocarbon barrier. An effective quasi-two-dimensional, transverse diffusion coefficient may be derived from the intercolumnar tunneling time using Eqn [10]:

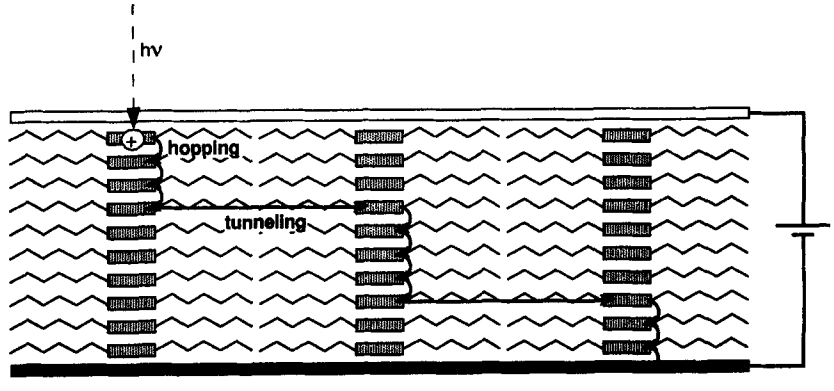

Figure 7 A schematic representation of orthogonally aligned PcOC*n* molecules functioning as a channeling charge transport layer. The transport time and temporal dispersion are controlled mainly by the intracolumnar jump time, τ_j. The lateral spatial dispersion is dependent on the ratio of τ_j to the intercolumnar tunneling time μ_T.

Table 3 Estimates of the charge carrier transit time t_D[a], dispersion parameter δ as given by Eqn [10] and inter-columnar tunneling probability, $P_T = t_D/\tau_T$

Compound	t_D (μs)	$\delta \times 10^6$	P_τ (%)
Crystalline solid			
PcOC6	0.05	19	25
PcOC9	0.03	0.9	0.9
PcOC12	0.04	0.2	0.2
PcOC8,2	0.03	18	20
Liquid crystal			
PcOC8,2[b]	0.2	2	2.0
PcOC8,2*	0.3	2	2.0
PcOC12,3	0.3	0.1	0.1
$[Si(PcOC8)O]_n$	0.2	0.04	0.1

[a] For an orthogonally aligned layer 1 μm thick with an applied potential of 1 V.
[b] Metastable mesophase at room temperature.

$$D_T \approx D^2/4\tau_T \quad [10]$$

in which D is the intercolumnar distance.

The degree of dispersion δ, may be expressed in terms of the ratio of the transverse to the longitudinal diffusion coefficients (Eqn [11]).

$$\delta = (\tau_J/2\tau_T)\,(D/d_J)^2 \quad [11]$$

For an isotropic medium $\tau_T = \tau_J$ and $D = d$ so that δ is 0.5. In Table 3, values of δ have been estimated using D from Table 1 and τ_J and τ_T in Table 2. As expected, the values are orders of magnitude lower than for an isotropic material.

A parameter which has a clearer physical significance is the probability that tunneling to an adjacent column will occur during drift. This is given simply by Eqn [12]

$$P_T \approx t_D/\tau_T \quad [12]$$

Values of P_T are also listed in Table 3. For the liquid-crystalline materials this probability amounts to, at most, only a few per cent for a 1 μm layer and a field of 1 V μm^{-1}. The lateral diffusion of charge carriers during drift should therefore be extremely small. Because of this, dispersion in the drift time will result mainly from one-dimensional diffusion within the columnar core as the charges traverse the layer.

Considering to a first approximation the electric field to be only a small perturbation on the normal diffusional motion, the root-mean-square diffusion distance, l_D, from the mean position will be

$$l_D = (2D_L t)^{1/2} \quad [13]$$

It is of importance for good temporal definition that l_D is small compared with the total drift distance. The ratio l_D/Δ can be obtained from Eqn [13] by substituting for $t = t_D$ from Eqn [6]. The result is simply

$$l_D/\Delta = (2k_B T/eV)^{1/2} \quad [14]$$

Temporal dispersion in the drift time, therefore, to a first approximation will be independent of the drift distance and the diffusion coefficient and dependent only on the applied voltage, for a given temperature. At room temperature, $k_B T = 0.025$ electron volts and l_D/Δ will be approximately 0.2 for a 1 V potential.

As a closing comment, it is considered unlikely that the fast transport times and extremely low lateral dispersions suggested by the data in Table 3 will be fully realizable in practice. The values do however provide at least an approximate quantitative insight into the expected behavior of discotic materials as charge transport layers and indicate performance targets at which it is possible to aim.

REFERENCES

1. S. Chandrasekhar, B. K. Sadashiva and K. A. Suresh, *Pramana.* **9**, 471 (1977).
2. S. Chandresekhar, *Rep. Prog. Phys.* **53**, 57 (1990).
3. S. Chandresekhar, *Mol. Cryst. Liq. Cryst.* **14**, 3 (1993).
4. C. Piechocki, J. Simon, A. Skoulios, D. Guillon and P. Weber. *J. Am. Chem. Soc.* **104**, 5245 (1982).
5. J. Simon and P. Bassoul. Phthalocyanine based liquid crystals: towards submicronic devices. In: *Phthalocyanines, Properties and Aplications,* Vol. II, Leznoff C. C. and Lever. A. B. P. (eds), VCH, New York, 1993, Chap. 6.
6. M. Hanack and M. Lang, *Adv. Mater.* **6**, 819 (1994).
7. G. Wegner, *Mol. Cryst. Liq. Cryst.* **235**, 1 (1993).
8. J. Simon and J.-J. André, *Molecular Semiconductors,* Springer, Berlin, 1985, Chapter III.
9. R. O. Loufty and Y. C. Cheng, *J. Chem. Phys.*, **73**, 2902 (1980).
10. N. N. Usov and V. A. Benderskii, *Phys. Status Solidi* **20**, 481 (1967).
11. N. Boden, R. J. Bushby and J. Clements, *J. Chem. Phys.* **98**, 5920 (1993).
12. G. Kruk, A. Kocot, R. Wrzalik, J. K. Vij, O. Karthaus and H. Ringsdorf, *Liq. Cryst.* **14**, 807 (1993).
13. D. Goldfarb, Z. Luz and H. Zimmermann, *J. Phys.* **42**, 1303 (1981).
14. A. M. Levelut, F. Hardouin, H. Gasparoux, C. Destrade and N. H. Tinh, *J. Phys.* **42**, 147 (1981).
15. W. Kranig, C. Boeffel and H. W. Spiess, *Macromolecules* **23**, 4061 (1990).

16. O. Karthaus, H. Ringsdorf, V. V. Tsukruk and J. H. Wendorf, *Langmuir* **8**, 2279 (1992).
17. E. Fontes, P. A. Heiney, M. Ohba, J. N. Haseltine and A. B. Smith III, *Phys. Rev. A* **37**, 1329 (1988).
18. D. Pressner, H. W. Glötner, H. W. Spiess and K. Müllen, *Ber. Busenges. Phys. Chem.* **97**, 1362 (1993).
19. P. G. Schouten, J. F. van der Pol, J. W. Zwikker, W. Drenth and S. J. Picken, *Mol. Cryst. Liq. Cryst.* **195**, 291 (1991) idem, *ibid.* **208**, 109 (1991).
20. E. Orthmann and G. Wegner, *Angew. Chem., Int. Ed. Engl.* **25**, 1105 (1986).
21. C. Sirlin, L. Bosio and J. Simon, *J. Chem. Soc., Chem. Commun.* 379 (1987) idem, *ibid.* 236 (1988).
22. T. Sauer and G. Wegner, *Mol. Cryst. Liq. Cryst.* **162B**, 97 (1988).
23. J. F. van der Pol, J. W. Zwikker, J. M. Warman and M. P. de Haas, *Recl. Trav. Chim. Pays-Bas* **109**, 208 (1990).
24. A. P. M. Kentgens, B. A. Markies, J. F. van der Pol and R. J. M. Nolte, *J. Am. Chem. Soc* **112**, 8800 (1990).
25. T. Sauer, *Macromolecules* **26**, 2057 (1993).
26. C. F. van Nostrum, A. W. Bosman, G. H. Gelinck, S. J. Picken, P. G. Schouten, J. M. Warman, A. J. Schouten and R. J. M. Nolte, *J. Chem. Soc., Chem. Commun.* 1120 (1993).
27. P. G. Schouten, J. M. Warman, M. P. de Haas, C. F. van Nostrum, G. H. Gelinck, R. J. M. Nolte, M. J. Copyn, J. W. Zwikker, M. K. Engel, M. Hanack, Y. H. Chang and W. T. Ford, *J. Am. Chem. Soc.* **116**, 6880 (1994).
28. D. D. Eley, *Mol. Cryst. Liq. Cryst.* **171**, 1 (1990).
29. T. J. Marks, *Angew. Chem., Int. Ed. Engl.* **29**, 857 (1990).
30. G. A. Cox and P. C. Knight, *J. Phys. C: Solid State Phys.* **7**, 146 (1974).
31. N. N. Usov and V. A. Benderskii, *Phys. Status Solidi* **B37**, 535 (1970).
32. D. Adam, P. Schumacher, J. Simmerer, L. Häussling, K. Siemensmeyer, K. H. Etzbach, H. Ringsdorf and D. Haarer, *Nature* (London), **371**, 141 (1994).
33. D. Adam, F. Closs, T. D. Frey, D. Funhoff, D. Haarer, H. Ringsdorf, P. Schuhacher and K. Siemensmeyer, *Phys. Rev. Lett.* **70**, 457 (1993).
34. D. Adam, D. Haarer, F. Closs, T. Frey, D. Funhoff, K. Siemensmeyer, P. Schuhmacher and H. Ringsdorf, *Ber. Busenges. Phys. Chem.* **97**, 1366 (1993).
35. P. M. Borsenberger and D. S. Weiss in: Handbook of *Imaging Materials*, Diamond, A. S. (ed), Dekker, New York, 1991, Chapter 9.
36. P. G. Schouten, J. M. Warman, M. P. de Haas, M. A. Fox and H.-L. Pan, *Nature* (London), **353**, 736 (1991).
37. P. G. Schouten, J. M. Warman, M. P. de Haas, J. F. van der Pol and J. W. Zwikker, *J. Am. Chem. Soc.* **114**, 9028 (1992).
38. P. G. Schouten, J. M. Warman, M. P. de Haas, H.-L. Pan and M. A. Fox, *Mol. Cryst. Liq. Cryst.* **235**, 115 (1993).
39. P. G. Schouten, PhD Thesis, University of Delft, The Netherlands, 1994.
40. J. F. van der Pol, J. W. Zwikker, R. J. M. Nolte and W. Drenth, *Recl. Trav. Chim. Pays-Bas* **107**, 615 (1988).
41. J. F. van der Pol, E. Neeleman, J. W. Zwikker, R. J. M. Nolte, W. Drenth, J. Aerts, R. Visser and S. J. Picken, *Liq. Cryst.* **6**, 577 (1989).
42. J. F. van der Pol. PhD Thesis, University of Utrecht, 1990.
43. J. M. Warman and M. P. de Haas. In: *Pulse Radiolysis of Irradiated Systems*, Tabata, Y. (ed.), CRC Press, Boca Raton, 1991, Chapter 6.
44. P. P. Infelta, M. P. de Haas and J. M. Warman, *Radiat. Phys. Chem.* **10**, 353 (1977).
45. P. G. Schouten, J. M. Warman and M. P. de Haas, *J. Phys. Chem.* **97**, 9863 (1993).
46. J. M. Warman, M. P. de Haas, J. F. van der Pol and W. Drenth, *Chem. Phys. Lett.* **164**, 581 (1989).
47. P. G. Schouten, J. M. Warman, G. H. Gelinck and M. J. Copyn, *J. Phys. Chem.* **99**, 11780 (1995).
48. A. O. Allen, National Bureau of Standards Report No. NSRDS–NBS 58, 1976.
49. J. Casanovas, R. Grob, D. Delacroix, J. P. Fuelfucci and D. Blanc, *J. Chem. Phys.* **75**, 4661 (1981).
50. J. Casanovas, R. Grob, R. Sabattier, J. P. Fuelfucci and D. Blanc, *Radiat. Phys. Chem.* **15**, 2936 (1980).
51. R. C. Alig, S. Bloom and C. W. Struck, *Phys. Rev. B*, **22**, 5565 (1980).
52. H. M. McConnell, *J. Chem. Phys.* **35**, 508 (1961).
53. M. J. Shephard, M. N. Paddon-Row and K. D. Jordan, *J. Am. Chem. Soc.* **116**, 5328 (1994).
54. C. Liang and M. D. Newton, *J. Phys. Chem.* **97**, 3199 (1993).
55. L. A. Curtiss, C. A. Naleway and J. R. Miller, *J. Phys. Chem.* **97**, 4050 (1993).
56. S. Larsson and M. Braga, *Chem. Phys.* **176**, 367 (1993).
57. K. Ohta, L. Jacquemin, C. Sirlin, L. Bosio and J. Simon, *New J. Chem.* **12**, 751 (1988).